Eur. Phys. J. B **43**, 195–200 (2005)
DOI: 10.1140/epjb/e2005-00042-6

THE EUROPEAN
PHYSICAL JOURNAL B

Strain-induced properties of epitaxial VO_x thin films

A.D. Rata[a] and T. Hibma

University of Groningen, Materials Science Centre, Nijenborgh 4, 9747 AG, Groningen, The Netherlands

Received 30 August 2004
Published online 25 February 2005 – © EDP Sciences, Società Italiana di Fisica, Springer-Verlag 2005

Abstract. We have grown VO_x thin films on different substrates in order to investigate the influence of epitaxial strain on the transport properties. We found that the electric conductivity is much larger for films grown under compressive strain on $SrTiO_3$ substrates, as compared to bulk material and VO_x films grown under tensile strain on MgO substrates. A clear crossover from metallic to semiconducting behavior is observed when increasing the oxygen content x. Apparently, the application of strain induces a Mott-Hubbard insulator-to-metal transition in $VO_{x<1}$. The $VO_x/SrTiO_3$ films show an unexpected large positive magnetoresistance effect at low temperatures, which is not found in the VO_x films grown under tensile strain on MgO or on a substrate with a similar lattice parameter.

PACS. 68.55.-a Thin film structure and morphology – 61.10.-i X-ray diffraction and scattering – 73.50.-h Electronic transport phenomena in thin films

1 Introduction

The physical properties of a transition metal oxide compound may be drastically modified by small changes of parameters like chemical composition, temperature and pressure. Illustrative examples of the effect of the first two factors are the manganese oxide perovskite compounds, where very rich phase diagrams are observed as a function of doping level and temperature [1,2]. Besides doping and temperature, pressure can also be employed to induce remarkable changes in the electronic structure and properties. For example, the transition temperature towards the superconductive state in $HgBa_2Ca_2Cu_3O_{8+\delta}$ increases from 133 K at ambient pressure to 164 K at 31 GPa [3].

Effects similar to those induced by high pressures, i.e., the modification of the crystalline and electronic structure, can be also attained by epitaxial growth. Epitaxial strain has a number of advantages over just hydrostatic pressure. By choosing the sign of the lattice mismatch between substrate and film, not only compressive, but also tensile stress can be applied. Secondly, a strain of a few percent can be easily realized by epitaxial growth as long as the thickness of the layer is smaller than the critical thickness for spontaneous dislocation. A strain of 2%, for example, corresponds to a pressure of about 10 GPa, which is comparable to the pressure reached with diamond anvil cells. There is of course a basic difference between epitaxial and hydrostatic strain. In epitaxial growth, the sample is allowed to expand or contract along the direction perpendicular to the surface. This implies that the unit cell of the film is slightly deformed, e.g., a cubic cell becomes tetragonal. This effect may also induce changes of certain physical properties of a transition metal compound.

Many examples of strain-induced modification of various physical properties of transition metal oxide compounds can be found in the literature. Recently Wang et al. [4] reported an enhancement of the room-temperature spontaneous polarization in epitaxial compressively strained thin films of the ferroelectric compound $BiFeO_3$. The crystal structure of these films was found to be monoclinic, in contrast to that of the bulk material which is rhombohedral. Bozovic et al. [5] observed that the critical temperature can be increased up to 40 K in La_2CuO_4 films under tensile strain with no Sr doping. Thin films of manganese oxide compounds have often a different Curie temperature and also an enhanced magnetoresistance coefficient as compared to the bulk material [1,6–8]. The electric conductivity of these films can be drastically modified by the substrate. For example, thin films of $La_{1-x}Sr_xMnO_3$ are metallic under tensile strain, whereas they become insulating under compressive strain [9].

Furthermore, epitaxial strain may give rise to new phases, not found in the bulk. For example, in $La_{0.67}Ca_{0.33}MnO_3$ films, Biswas et al. [10] reported the existence of a strain-driven low-temperature charge-ordered insulating state which is not observed in bulk samples. Different phases than those corresponding to the bulk material are sometimes observed in binary transition metal oxide thin films. Examples are Cr_xO epitaxially grown on substrates having a cubic lattice [11], $Fe_{1-x}O_{1-y}N_y$, an oxynitride in which oxygen has been replaced by up to 25% of nitrogen [12] and the γ phase of Fe_2O_3, which can be stabilized on a cubic substrate such as MgO [13]. We

[a] e-mail: d.rata@fz-juelich.de

note that these are metastable phases stabilized by interface interactions.

In this paper we investigate the possibility of "tuning" the structural, electric and magnetic properties of epitaxially grown VO_x films via strain-induced effects by different substrates. VO_x was chosen as a model system because within the first-row transition metal monoxides is known to be at the brink of metallic and insulating behavior. The use of epitaxial strain induced by the substrate makes it possible to modify several properties of bulk VO_x and, when changing the substrate, even to obtain a "fine tuning" of some of these properties. First, we have chosen $SrTiO_3$, since this substrate has a smaller lattice constant, $a = 3.905$ Å. The lattice constant of bulk VO_x is 4.06 Å [14]. The VO_x films may be thus "forced" to grow under compressive strain. The electric properties of these films are compared to previously published data for films grown under tensile strain on MgO ($a = 4.213$ Å) [15] and those of virtually unstrained films grown on $MgAl_2O_4$ ($a = 8.083$ Å). We will show that the conductivities for the same oxygen content x are very different.

2 Experimental

VO_x films with a thickness of 100 Å were grown in situ by Molecular Beam Epitaxy (MBE) on $SrTiO_3$(100) (STO) and $MgAl_2O_4$(100) (MAO) substrates. The STO substrates were annealed in vacuum at 500 °C whereas the MAO substrates were cleaned at 600 °C in an oxygen atmosphere. Vanadium metal was deposited at room temperature and simultaneously oxidized by a controlled beam of $^{18}O_2$. The stoichiometry of the VO_x films was determined using the ^{18}O - RBS (Rutherford backscattering spectrometry) method [15]. The structure was characterized in situ using reflection high-energy electron diffraction (RHEED) and ex situ by X-ray diffraction (XRD). The transport measurements were performed in a commercial Quantum Design PPMS system, in the standard four-point geometry for temperatures between 4 and 300 K. Four electrical contacts of Cr metal, 10 nm thick and 1 mm wide, were evaporated on each substrate prior to deposition of the VO_x layers. After deposition of the VO_x films the contacts are stable, no non-linear current-voltage characteristics were ever found. All ex situ measurements, i.e., XRD, RBS and conductivity measurements, were performed on VO_x samples capped with a thin MgO layer ($\simeq$20 Å) as protection against postoxidation.

3 Results and discussion

3.1 Structural characterization

In a previous report we showed that VO_x grows epitaxially on MgO(100) substrates with the same rocksalt crystal structure, see reference [15]. In this paper we show that epitaxial growth can also be obtained on STO(100) substrates with a cubic perovskite structure and a smaller lattice constant. The lattice mismatch is approximately 4%. The epitaxial growth of rocksalt VO_x films on perovskite-type STO substrates was confirmed by RHEED and XRD analysis. The quality of the films was excellent, the RHEED and XRD measurements showing very high crystallinity and the absence of any secondary phases.

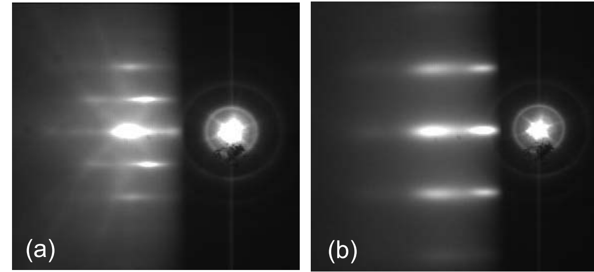

Fig. 1. RHEED patterns recorded at an electron energy of 15 kV with the beam incident along the [100] direction: (a) clean STO(100) substrate; (b) 100 Å VO_x (100) thin film on a STO(100) substrate.

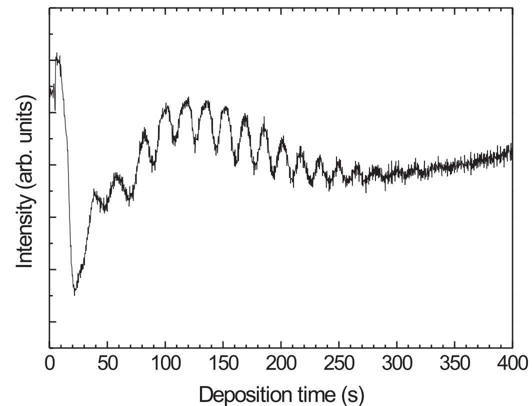

Fig. 2. RHEED intensity oscillations of the specularly reflected electron beam observed during deposition of VO_x on STO(100). The electron beam was incident along the [100] direction, with a primary energy of 15 kV.

In Figure 1a we show the RHEED pattern of a clean STO(100) surface and in Figure 1b the RHEED pattern of a 100 Å thick VO_x film deposited on STO(100). One can clearly notice the difference between the perovskite structure of the clean substrate, where the (10) and ($\bar{1}$0) diffraction lines are present, and the rocksalt structure of the film, with only the (20) and ($\bar{2}$0) lines visible. The oscillations in the intensity of the specularly reflected beam observed during growth are characteristic for a *layer-by-layer* growth mechanism. An example of such growth oscillations is shown in Figure 2.

The epitaxial growth of the rocksalt VO_x film on the STO substrate was further confirmed by ex situ XRD. All XRD measurements were carried out on capped samples. In Figure 3 a wide θ–2θ scan is shown. Only the (002) and (004) diffraction peaks of the film were observed, indicating that the VO_x film grows with a rocksalt structure on top of the perovskite $SrTiO_3$ substrate.

The growth of the VO_x films on STO substrates is coherent, i.e., the in-plane lattice matches with that of the substrate. In Figure 4 we show an XRD reciprocal space

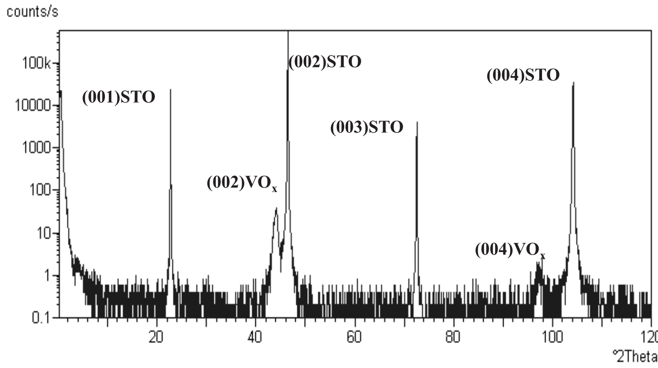

Fig. 3. $\theta - 2\theta$ X-ray diffraction measurements on a 10 nm thick VO_x film. Only the (002) and (004) diffraction peaks, indicating a rocksalt structure, of the VO_x film are observed. No diffraction peaks are observed close to the (001) and (003) peaks of the perovskite STO substrate. Reflections from the VO_x film are broadened due to the finite thickness.

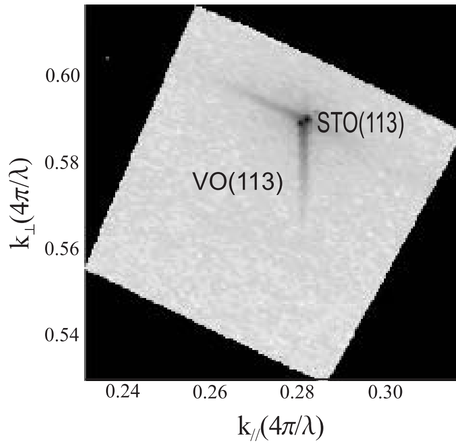

Fig. 4. XRD reciprocal space map around the non-specular (113) reflection for a 10 nm thick VO_x film. The diffracted intensity as function of the in-plane $k_{\|}$ and out-of-plane $k_{\perp}$ reciprocal lattice vectors is plotted on a logarithmic scale. The axes are in units of $4\pi/\lambda$, with $\lambda = 0.15015$ nm.

map around the non-specular (113) reflection of a 10 nm thick VO_x film. The intensity scale in the figure is logarithmic. The horizontal and vertical axes are k-vectors parallel ($k_{\|}$) and perpendicular ($k_{\perp}$) to the surface plane, respectively. The feature corresponding to the VO_x film can be clearly distinguished. The elongated shape of the STO reflection perpendicular to the radial direction is due to the mosaic spread. The peaks of the STO substrate and of the VO_x film are at the same $k_{\|}$ value, which proves that the growth is fully coherent. Compared to the VO_x films grown on MgO under tensile strain, discussed in reference [15], the VO_x films grown on STO substrates experience a compressive in-plane strain. In Section 3.3 we will discuss the influence of this compressive strain on the electric properties.

The lattice constant normal to the surface can be calculated from $\theta - 2\theta$ scans around the (002) or (004) peaks

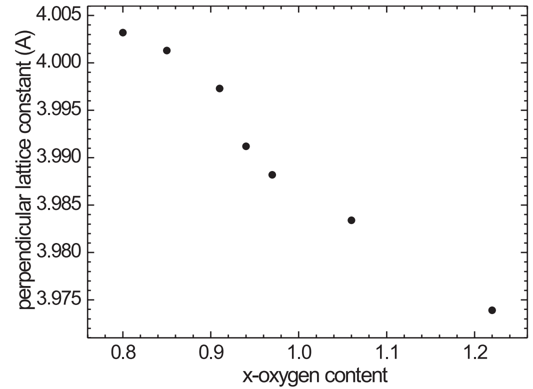

Fig. 5. Perpendicular lattice constant as a function of the oxygen content x as determined from XRD.

of the STO substrate by using the Bragg law. The perpendicular lattice constant is shown in Figure 5, plotted as a function of the oxygen content. Just like in the case of films grown on MgO, the lattice constant in the perpendicular direction, and consequently the average lattice constant, decreases with increasing oxygen content. The thickness of the films was also determined from X-ray specular reflectivity (XRR) measurements and confirmed the values estimated from the RHEED intensity oscillation period.

3.2 Oxygen content x in VO_x films on $SrTiO_3$

The method employed to determine the oxygen content of our VO_x films was described in reference [15]. Because vanadium ions in different oxidation states have rather similar values of the V $2p_{3/2}$ binding energy, which makes XPS rather ineffective as a method to determine the stoichiometry, we employed the ^{18}O - RBS technique. This was found to be very convenient, because the use of $^{18}O_2$ instead of $^{16}O_2$ for film preparation enables one to make a clear distinction between the oxygen corresponding to the film and to the substrate, respectively. We present in Figure 6 the RBS spectrum of a VO_x film grown on a STO substrate. Using a V_2O_3 film grown epitaxially on Al_2O_3 as calibration sample, the x values for a series of VO_x/STO samples were calculated from the following simple relation

$$x = \frac{3}{2} \frac{[\frac{A_O}{A_V}]_{VO_x}}{[\frac{A_O}{A_V}]_{V_2O_3}} ,$$

and plotted in Figure 7. A_O and A_V were determined by integrating the V and ^{18}O peaks of the VO_x and V_2O_3 samples. The upper and lower limits of stoichiometry are similar to those obtained for the VO_x films grown on MgO and also to the values known for the bulk compound [14]. For these determinations we estimated a relative error of about 3%.

A peculiar characteristic of the VO_x system is the presence of a large number of both anion and cation vacancies. From the period of the RHEED intensity oscillations, which gives the time needed to grow one monolayer of VO_x and V_2O_3, respectively, we can calculate the fraction of vacant vanadium sites (V_V) in VO_x, assuming that

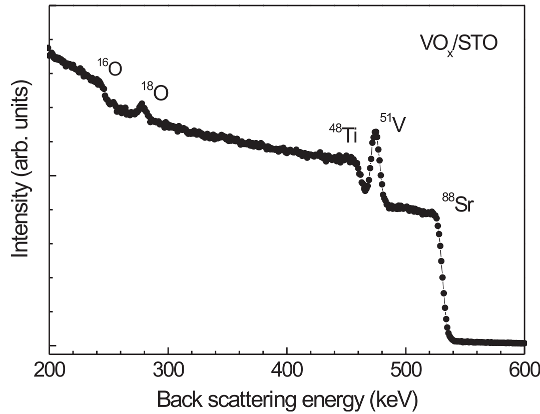

Fig. 6. RBS spectrum of a VO_x film grown on STO(100) substrate.

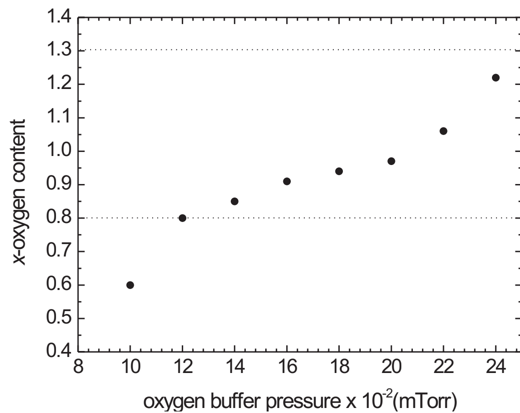

Fig. 7. Oxygen content x for a series of VO_x films as determined from RBS.

V_2O_3 is stoichiometric and free of vacancies. The oxygen vacancy concentration (V_O) can also be obtained, once we know the oxygen content x, see reference [15]. We found that the concentration of oxygen and vanadium vacancies in VO_x films grown under tensile strain on MgO do not differ much from the values in the bulk [15]. The fact that the number of vacancies is rather strain-insensitive is also confirmed for the $VO_{x\geq1}$/STO samples but not for the case of $VO_{x<1}$/STO samples. In Figure 8 we show the concentration of both vanadium and oxygen vacancies determined from the RHEED and RBS data. The same trend is observed for VO_x on STO as for VO_x on MgO, i.e., the number of oxygen vacancies decreases with increasing x, while the concentration of vanadium vacancies increases with increasing x.

3.3 Transport properties

The most significant effect of the epitaxial strain was observed on the transport properties. It was shown that VO_x epitaxially grown on MgO under tensile strain displays a much lower electric conductivity than bulk samples [15]. This was explained in terms of a smaller orbital overlap in the coherently tensile strained layers. Consistently, we found that the compressively strained VO_x films on STO have higher conductivity. The VO_x films grown

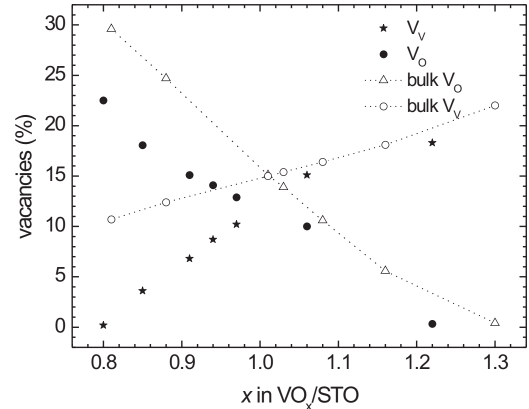

Fig. 8. Vanadium and oxygen vacancy concentrations in VO_x as determined from the period of the RHEED oscillations. The amount of vanadium vacancies increases with x, while the concentration of oxygen vacancies decreases. Dotted lines correspond to the data for the bulk material, as reported by Banus et al. [14].

on MgO are mostly semiconducting-like; the gradual transition from metallic to semiconducting behavior is shifted from $x=1$ in bulk to 0.82 in the VO_x/MgO thin films, see Figure 9a. Under compressive strain, the transition from metallic to semiconducting behavior is much more clear, see Figure 9c. The resistivity of the $VO_x=0.94$/STO sample is temperature independent. For $x<0.94$ the VO_x films grown on STO show real metallic conductivity, in the sense that the resistivity decreasing with decreasing temperature. The metallic samples have a very low residual resistivity, between 10^{-5} and 10^{-6} Ωcm at 5 K, the lowest temperature employed. I has been brought to our attention by one of the referees of this paper, that this low resistivity might be due to the STO substrate instead of the VO_x film, because STO can become metallic or even superconducting, if annealed at high temperatures, e.g. between 700 and 900 °C, under appropriate reducing conditions [16]. However, as described in the experimental part, our STO substrates were only annealed at 500 °C. The resistivity of the annealed substrates was found to be larger than 2 GΩ between 10 K and room temperature. Therefore, we can exclude the influence of the substrate on the measured conductivity of the VO_x films. Another indication that the observed resistivity can not be due to the substrate, is the observation that the resistivity data depend in a systematic way on the composition, e.g. oxygen content (see Fig. 9).

We have also prepared a series of VO_x films using $MgAl_2O_4$ as a substrate. $MgAl_2O_4$ has a spinel crystal structure. However, epitaxial growth with a rocksalt configuration is possible because both crystal structures are based upon a *fcc* oxygen lattice. The continuity of the oxygen sublattice may be thus preserved at the $MgAl_2O_4/VO_x$ interface. The lattice constant of $MgAl_2O_4$ is 8.083 Å [17], which gives a very small lattice mismatch of about 0.5%. By RHEED and XRD measurements we found that the VO_x layers grow indeed epitaxially on $MgAl_2O_4$ and have a rocksalt structure. The oxygen content in these series of samples was determined by

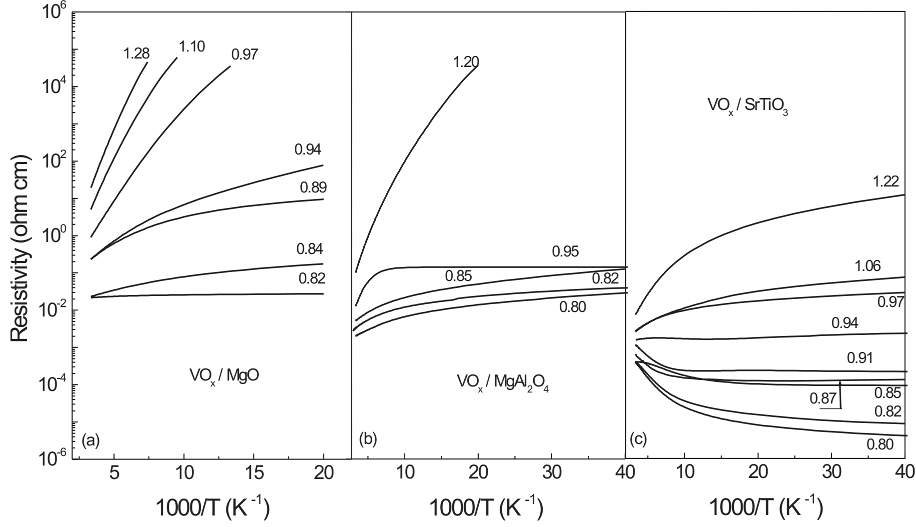

Fig. 9. Resistivity of 100 Å thick VO_x films with different oxygen content x grown on: (a) MgO, under tensile strain; (b) $MgAl_2O_4$, nearly strain free; (c) $SrTiO_3$, under compressive strain.

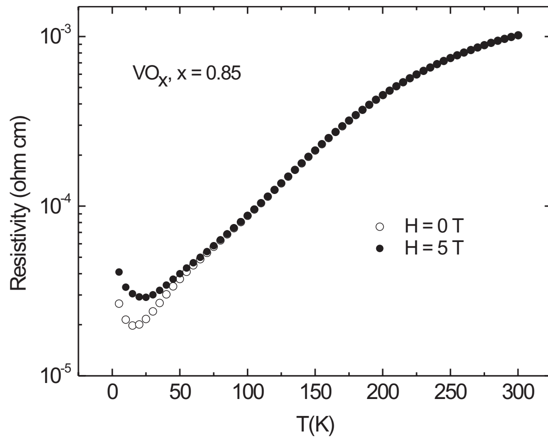

Fig. 10. The resistivity of a 100 Å thick VO_x film with $x = 0.85$ at zero field and at $H = 5$ T.

$^{18}O_2$ - RBS measurements in the same way as described in the previous section.

The temperature dependence of the resistivity is illustrated for several VO_x/MAO samples in Figure 9b. For similar oxygen content x the conductivity of the VO_x/MAO films takes intermediate values between the values corresponding to films grown on MgO (Fig. 9a) and $SrTiO_3$ (Fig. 9c). The results of our measurements on the VO_x on MAO samples are very similar to the data reported by Banus et al. [14] for bulk material. An important difference in the resistivity behavior was observed for the metallic samples grown under compressive strain on STO. In Figure 10 we show the temperature dependence of the resistivity for the $x = 0.85$ film at temperatures between 5 and 300 K. The resistivity strongly decreases with decreasing temperature, reaches a minimum of $\approx 2 \times 10^{-5}$ Ωcm at $T = 20$ K, and increases steeply at temperatures below 20 K. In the same figure we compare the temperature dependence of the resistivity of the VO_x film in zero magnetic field with that measured in an external field of 5 T. As to the field dependence, the two curves, $\rho(T, H = 0)$ and $\rho(T, H = 5$ T$)$, are indistinguishable down to $\simeq 70$ K. At lower temperatures the application of a magnetic field increases the resistivity. The positive magnetoresitance effect observed in our films is strongly dependent on the oxygen content. The effect is largest in the sample with the smallest oxygen content, $x = 0.80$, where the magnetoresistance coefficient amounts to 70% at a temperature of 5 K and a magnetic field of 5 T. For higher x oxygen content the magnetoresistance decreases and finally becomes unobservable for $x > 0.94$, in an apparent correlation with the crossover from the metallic to the semiconducting regime [18]. The magnetoresitance coefficient was negligible in the case of VO_x films epitaxially grown on MgO and MAO substrates.

4 Discussion

It is evident from the results presented in the previous section that epitaxial strain has a very strong impact on the electronic conductivity of vanadium monoxide. The valence electronic structure itself is actually modified as a result of this lattice mismatch between film and substrate. At low temperatures the differences for samples having the same composition are many orders of magnitude. Under a tensile lateral strain the behavior is semiconducting-like for the higher x values with an activation energy of up to 0.2 eV and of the variable range hopping type for intermediate x values, with the resistivity curves showing a $T^{-1/4}$ dependence [15]. Under compressive strain, the the low-x samples are metallic, i.e. the resistivity decreases with temperature, reaching values as low as $\sim 10^{-5}$ Ωcm. Intuitively, this huge change is related to an increase of the direct overlap between the t_{2g} valence orbitals in the

compressed films, but the precise mechanism cannot be formulated in a straightforward way. As explained in a classical papers by Goodenough [19] and Mott [20] the electronic structure of the monoxides of vanadium and titanium is affected by the presence of very large numbers of vacancies of both kinds and in the case of VO by strong correlation effects. The main ingredients of their description of the electronic structure of the early transition metal monoxides are the direct electron transfer between the partly occupied t_{2g} orbitals and the on-site Coulomb repulsion U. Strain modifies the transfer integral but leave the Hubbard U unchanged. In the case of VO_x apparently the Hubbard gap is opened up under tensile strain and fully closed under compressive strain. In other words, the application of strain induces a Mott-Hubbard insulator-to-metal transition in $VO_{x<1}$. This is not unexpected because similar transitions are observed in V_2O_3 and VO_2.

In the case of coherent layers of VO_x on MgO the cation and anion vacancy concentrations are very similar to those in bulk material [15]. This is also true for the coherent layers on STO presented in this paper for x values above approximately 1. However, for the metallic layers on STO with low x values, the number of vacancies is lower for both kinds. This is particularly evident for the oxygen vacancy concentration of films with an x value of 0.8, which is virtually zero as compared to about 10% for bulk samples. In order to explain the stability of these large numbers of vacancies, Goodenough argued that the formation of vacancies is favorable since the resulting contraction of the lattice yields more direct overlap between t_{2g} orbitals. As we discussed extensively in the case of VO_x layers on MgO [15], this implies a strong effect of strain on vacancy concentration, which is not observed in the VO_x/MgO case. However, it seems that Goodenough's arguments might apply to the metallic samples, because we found that vacancies are removed in the compressively strained films. The peculiar upturn of the resistivity and concomitant giant magneto-resistance effect in the metallic samples are most probably related to localization and strong electron-electron interaction effects in a strongly disordered metal, the disorder being caused by the presence of vast numbers of vacancies as discussed in reference [18].

5 Conclusions

In summary, we have grown epitaxial VO_x films on different substrates, in order to investigate the influence of epitaxial strain on the transport properties. RHEED and XRD measurements indicate a high quality of the VO_x films. The oxygen content x was determined for each film using ^{18}O - RBS and the amount of vacancies was estimated by combining RHEED and RBS techniques. In order to avoid size effects we prepared films with the same thickness. The presence of epitaxial strain is strongly reflected in the magneto-electric properties. VO_x films grown under compressive strain on $SrTiO_3$ exhibit higher conductivity as compared to VO_x films grown under tensile strain on MgO. As expected, using $MgAl_2O_4$ substrates with a lattice constant comparable to VO, the conductivity is much closer to the bulk values and in-between the values obtained for films grown on $SrTiO_3$ and MgO. Apparently, the Hubbard gap is opened up under tensile strain and fully closed under compressive strain. VO_x films grown under compressive strain show a large positive magnetoresistance effect, which is not present in the films grown under tensile strain or on a substrate with a similar lattice parameter.

We would like to thank D. Borsa for the help with the RBS measurements and T.T.M. Palstra for the possibility of using his equipment.

References

1. M.B. Salamon, M. Jaime, Rev. Mod. Phys. **73**, 583 (2001)
2. E. Dagotto, T. Hotta, A. Moreo, Phys. Rep. **344**, 1 (2001)
3. L. Gao, Y.Y. Xue, F. Chen, Q. Xiong, R.L. Meng, D. Ramirez, C.W. Chu, J.H. Eggert, H.K. Mao, Phys. Rev. B **50**, 4260 (1994)
4. J. Wang, J.B. Neaton, H. Zheng, V. Nagarajan, S.B. Ogale, B. Liu, D. Viehland, V. Vaithyanathan, D.G. Schlom, U. V. Waghmare, N.A. Spaldin, K.M. Rabe, M. Wuttig, R. Ramesh, Science **299**, 1719 (2003)
5. I. Bozovic, G. Logvenov, I. Belca, B. Narimbetov, I. Sveklo, Phys. Rev. Lett. **89**, 107001 (2002)
6. D. Kumar, R.K. Singh, C.B. Lee, Phys. Rev. B **56**, 13666 (1997)
7. T.Y. Koo, S.H. Park, K.B. Lee, Y.H. Jeong, Appl. Phys. Lett. **71**, 977 (1997)
8. R.A. Rao, D. Lavric, T.K. Nath, C.B. Eom, L. Wu, F. Tusi, Appl. Phys. Lett. **73**, 3294 (1998)
9. Y. Konishy, Z. Fang, M. Izumi, T. Manako, M. Kasay, H. Kuwahara, M. Kawasaki, K. Terakura, Y. Tokura, J. Phys. Soc. Jpn **68**, 3790 (1999)
10. A. Biswas, M. Rajeswari, R.C. Srivastava, T. Venkatesan, R.L. Greene, Q. Lu, A.L. de Lozanne, A.J. Millis, Phys. Rev. B **63**, 184424 (2001)
11. Actually CrO does not exist as bulk crystal, see O.C. Rogojanu, Ph. D. thesis, University of Groningen, 2002
12. F.C. Voogt, P.J.M. Smulders, G.H. Wijnja, L. Niesen, T. Fujii, M.A. James, T. Hibma, Phys. Rev. B **63**, 125409 (2001)
13. F.C. Voogt, T. Fujii, P.J.M. Smulders, L. Niesen, M.A. James, T. Hibma, Phys. Rev. B **60**, 11193 (1999)
14. M.D. Banus, T.B. Reed, A.J. Strauss, Phys. Rev. B **5**, 2775 (1972)
15. A.D. Rata, A.R. Chezan, T. Hibma, M.W. Haverkort, L.H. Tjeng, H.H. Hsieh, H.-J. Lin, C.T. Chen, Phys. Rev. B **69**, 075404 (2004)
16. J.B. Philipp, D. Reisinger, M. Schonecke, M. Opel, A. Marx, A. Erb, L. Alff, R. Gross, J. Appl. Phys. **93**, 6853 (2003)
17. C.N.R. Rao, B. Raveau, *Transition Metal Oxides* (VCH Publishers, New York 1995), p. 121
18. A.D. Rata, V. Kataev, D. Khomskii, T. Hibma, Phys. Rev. B **68**, 220403 (2003)
19. J.B. Goodenough, Phys. Rev. B **5**, 2764 (1972)
20. N.F. Mott, Phyl. Mag. **24**, 935 (1971)